Czech Phycological Society

*Fottea, 26*(2), 140–155, 2026
doi: 10.5507/fot.2026.001

# Cryptic diversity in the marine diatom genus *Climaconeis* (Berkeleyaceae, Bacillariophyta) with description of *Climaconeis aucklandensis sp. nov.*

Rinat M. Gogorev[1], Olga Davidovich[2], Nickolai Davidovich[2], Yekaterina Bedoshvili[3], Vyacheslav Yu. Nikulin[4], and Arthur Yu. Nikulin[4]

**Abstract**

Clonal cultures of the diatom genus *Climaconeis* from the Black Sea (Crimea), Mediterranean Sea (Anatolia), Atlantic Ocean (Canary Islands), and Southwest Pacific Ocean (Auckland, New Zealand) were investigated. The Auckland population is described as *Climaconeis aucklandensis* sp. nov., distinguished by 4–12 H-shaped plastids per cell, a larger valve size range, and different stria density. We used morphological (LM, SEM, TEM, LSM), molecular (*rbc*L), and ecophysiological (salinity tolerance) analyses to characterize *C. aucklandensis*, *C. scalaris*, and *Climaconeis* cf. *scalaris*. Black Sea and Atlantic specimens resembled *C. scalaris* but differed diagnostically. New Zealand strains were morphologically close to *C. undulata* but genetically distinct. Sexual compatibility was confirmed between Black Sea and Mediterranean populations. Three species delimitation methods (ASAP, PTP, GMYC) identified six genetic lineages, supporting significant cryptic diversity within the genus.

**Keywords**

*Climaconeis aucklandensis*, *Climaconeis scalaris*, morphology, plastids, raphid naviculoid diatoms, *rbc*L phylogeny, taxonomy

[1] *Laboratory of Algology, Komarov Botanical Institute, Russian Academy of Sciences, St. Petersburg, 197022, Russia*
[2] *T.I. Vyazemsky Karadag Scientific Station – Nature Reserve of RAS – Branch of A.O. Kovalevsky Institute of Biology of the Southern Seas, Russian Academy of Sciences, Feodosia, 298188 Russia*
[3] *Limnological Institute, Siberian Branch, Russian Academy of Sciences, Irkutsk, 664033, Russia*
[4] *Federal Scientific Center of the East Asia Terrestrial Biodiversity, Far Eastern Branch of the Russian Academy of Sciences, Vladivostok, 690022, Russia*

**Corresponding author**
Nickolai Davidovich
nickolaid@yandex.ru

**Article History**
*Received July 30, 2025*
*Revised November 18, 2025*
*Accepted January 1, 2026*
*Published online September 9, 2026*

**Supplementary Material**
*Available online*

**How to cite**
Gogorev, R. M., Davidovich, O., Davidovich, N., Bedoshvili, Y., Nikulin, V. Yu., & Nikulin, A. Yu. (2026). Cryptic diversity in the marine diatom genus *Climaconeis* (Berkeleyaceae, Bacillariophyta) with description of *Climaconeis aucklandensis sp. nov. Fottea*, *26*(2), 140–155. https://doi.org/ 10.5507/fot.2026.001

## Introduction

The genus *Climaconeis* Grunow was resurrected by Cox (1982), who provided an amended description of the genus along with an identification key to six of its species. *Climaconeis* was placed in the family Naviculaceae, with the presence of H-shaped plastids serving as an important diagnostic feature. After examining several species previously classified by various authors under the genera *Navicula* Bory, *Amphipleura* Kützing, *Frustulia* C.A. Agardh, *Okedenia* Eulenstein *ex* De Toni, *Denticula* Kützing, *Climacosphenia* Ehrenberg, and *Stichodesmis* Greville, as well as resolving several intricate nomenclatural problems, Cox placed six species in *Climaconeis* and designated *Climaconeis lorenzii* Grunow as the type species. A further description of the genus was presented by Round *et al*. (1990).

*Climaconeis* species are epipelic marine diatoms characterized by multiple paired H-shaped plastids per cell. The valves are elongate and linear, with obtuse or capitate apices. The raphe may be straight or biarcuate, terminating before reaching the apices and potentially deflecting to one side at the center. The raphe-sternum is sometimes thickened, and prominent helictoglossae occur at the poles. The striae are parallel and consist of simple areolae.

As Lobban *et al*. (2012) noted, the prospect for new species is evident in the small genus *Climaconeis* Grunow emend. E.J. Cox. Recently, twelve tropical species have been described from Florida (Prasad, 2003; Prasad *et al.,* 2000), Abu Dhabi (Reid & Williams, 2002), Guam (Lobban, 2018; Lobban *et al.,* 2010, 2012), Korea (Park *et al.,* 2016) and Marshall Islands, Micronesia (Lobban, 2021). The total number of currently recognized species increased to

22 (Guiry & Guiry, 2025), of which only three were found in temperate waters (Reid & Williams, 2002) and only two described or found in south hemisphere from Australia (John, 1991) and New Zealand (Harper *et al.,* 2012).

Cox (1982) and Prasad *et al.* (2000) summarized the taxonomic history of the genus and Lobban *et al.* (2012) discussed the short history of plastids, which are a significant feature in the genus taxonomy. As Lobban *et al.* (2012) noted, most species are readily recognized in living material by the presence of a series of several to many large plastids, which are described as H-shaped with a central pyrenoid (Cox, 1979; Prasad *et al.,* 2000). The history of the H-shaped plastid dates back to Mereschkowsky (1901a, 1901b, 1903) who gave priority to the form and structure of plastids, calling them internal features, rather than the form and structure of frustules, calling them external ones. Other significant characters should be mentioned, *Climaconeis* frustules can be curved or straight and some "straight" species have craticular bars on the valvocopula.

During a survey of the diatom flora in the algal mats associated with stromatolites in Hamelin Pool, Shark Bay, Western Australia, large numbers of a *Climaconeis*-associated diatom were encountered. The diatom observed was reported as *Climaconeis* aff. *scopulorioides* (Hustedt) E.J.Cox (John, 1991).

The paper aims to study the biology, morphology, taxonomy, and phylogenetic position of three cryptic *Climaconeis* taxa and to describe a new species based on morphological, molecular, and ecophysiological data. Based on available published data on all species of the genus three sections are proposed, as well as emended diagnoses of species studied are presented.

## Materials and Methods

Samples were collected from the upper sublittoral zone at a depth of 0.2–0.5 m as epilithic biofilm scrapings. Details of sampling locations, coordinates, and dates are summarized in Table 1.

Clones were isolated by micropipette and placed in glass Petri dishes filled with approximately 40 ml of ESAW culture medium (Andersen *et al.,* 2005, p. 494). Cultures were maintained at 20±2°C under natural light (from north-facing windows to avoid direct sunlight). Exponential growth was sustained by weekly reinoculation into fresh medium. Live stages were observed using NIB-100 (Delta Optical, China) and Biolar PI (PZO, Poland) light microscopes equipped with bright field (BF) or differential interference contrast (DIC) optics. Images were acquired with a Canon PowerShot A640 digital camera. Cell sizes were measured using the acquired images and ImageJ software (https://imagej.nih.gov/ij/). For scanning electron microscopy (SEM), cells were cleaned by boiling in concentrated hydrogen peroxide ($H_2O_2$); the cell suspension was centrifuged at a relative centrifugal force of about 200 g and rinsed with distilled water 5–7 times, air-dried on an aluminum stub, sputter-coated with gold, and observed with a Jeol JSM-6390LA (JEOL, Japan) scanning electron microscope.

**Molecular analysis**: For DNA analysis, the unialgal cultures were harvested during the exponential growth phase and concentrated by centrifugation. Total genomic DNA was extracted according to Abdullin *et al.* (2021). PCR amplification of the plastid-encoded *rbc*L gene region was carried out using primers DPrbcL1 (5'-AAGGAGGAADHHATGTCT-3') and DPrbcL7 (5'-AAASHDCCTTGTGTWAGTYTC-3', Daugbjerg & Andersen, 1997) with the Encyclo Plus PCR kit (Evrogen, Moscow, Russia). The PCR products were purified using ExoSAP-IT PCR Product Cleanup Reagent (Affymetrix, Santa Clara, CA, USA) and sequenced in both directions using an ABI 3500 genetic analyzer (Applied Biosystems, Foster City, California, USA) at the Instrumental Center of Biotechnology and Gene Engineering of FSCEATB, FEB RAS with a BigDye terminator v3.1 Sequencing kit (Life Technologies Corporation, Austin, TX, USA) and the same primers used for PCR. Sequences were assembled with the Staden Package v. 1.4 (Bonfield *et al.,* 1995).

The dataset was enriched by all available *Climaconeis* sequences in GenBank. The sequences (taxa and accession numbers are given in the tree) were aligned using SeaView (Galtier *et al.,* 1996). Phylogenetic analyses were performed using

**Table 1**. Locations of periphyton sampling sites.

| Location | Sea/Region | Coordinates | Sampling Date | Salinity (‰) | Isolated clones |
|---|---|---|---|---|---|
| Auckland Harbour, New Zealand | Southwest Pacific Ocean | 36°50'28.32"S, 174°45'33.39"E | May 2015 | 36 | 5.0630-OC<br>5.0630-OD<br>5.0703-OB<br>5.0703-OK |
| Crimean Peninsula | Black Sea | 44°54'40.7"N, 35°12'48.3"E | July 2015 | 18 | 5.0716-OA (=SZCZ 1888) [1]<br>8.0118-OA [2] |
| Tenerife, Canary Islands | Atlantic Ocean | 28°01'40.3"N 16°35'33.2"W | May 2018 | 36 | 8.0601-OA (=SZCZ 1889) [1]<br>8.0601-OB |
| Kızılot coast, Turkey | Mediterranean Sea | 36°42'30.1"N 31°33'59.8"E | August 2023 | 40 | 23.0820-OA<br>23.0820-OB<br>23.0820-OD<br>23.0820-OE |

Note: [1] synonymous strain number in the collection of the University of Szczecin (Poland); [2] F1 progeny resulted from mating parental clones 5.0720-Z + 5.0716-D.

*Fottea, 26*(2), 140–155, 2026
doi: 10.5507/fot.2026.001

sequences from *Neidium* Pfitzer (Neidiaceae) as an outgroup, a taxon phylogenetically distant from the ingroup yet within the same order (Naviculales). To determine the most appropriate DNA substitution model for the datasets, we applied the Akaike information criterion (AIC; Akaike, 1974) using jModelTest 2.1.1 (Darriba *et al.,* 2012). The GTR+I model was selected as the best fit for the dataset. Phylogenetic trees were constructed using maximum likelihood (ML) in IQ-TREE 2 (Minh *et al.,* 2020) and Bayesian inference (BI) in MrBayes v.3.1.2 (Ronquist & Huelsenbeck, 2003). For BI, four runs of four Markov chains were executed for 1 million generations, sampling every 100 generations for a total of 10,000 samples. Convergence of the chains was assessed, and stationarity was determined according to the 'sump' plot with the first 25% of samples were discarded as burn-in; posterior probabilities were calculated from remaining. The convergence of the stationary distribution was accessed by ESS values (>200) using Tracer v.1.7.1 (Rambaut *et al.,* 2018). The support values for the ML trees nodes were estimated using ultrafast bootstrap (1000 replicates; bootstrap percentages (BP); Hoang *et al.,* 2018) and posterior probabilities (PP) in BI. BP < 70% and PP < 0.95 were not considered. Pairwise distances (*p*-distances) were estimated using MEGA 11 (Tamura *et al.,* 2021).

The *rbc*L dataset was applied for species delineation using the Assemble Species by Automatic Partitioning (ASAP) method (Puillandre *et al.,* 2021), accessed via the online service https://bioinfo. mnhn.fr/abi/public/asap/asapweb.html. The ML tree was employed to delineate putative species by a maximum likelihood Poisson tree processes (PTP) model (Zhang *et al.,* 2013). This analysis was conducted using an online service https://species.h-its.org/. The generalized mixed Yule coalescent (GMYC) method (Fujisawa & Barraclough, 2013) with the online service https://species.h-its.org/gmyc, was used to select clusters at the species level on the tree and to determine the species delimitation threshold. The ultrametric phylogenetic tree for the GMYC analysis was reconstructed by the Bayesian method in the BEAST v1.10.4 program (Drummond & Rambaut, 2007) with an uncorrelated relaxed lognormal molecular clock. During phylogenetic reconstruction, the number of generations for Markov chains was set to ten million.

**Salinity factor**: The effect of salinity on the algae was estimated by their growth rate. For more than one year, clones from Crimea were maintained in culture at a salinity 20‰ while clones from Tenerife and New Zealand were kept at 36‰, the levels approximated to their natural habitats. Periodically (once per month), clones were reinoculated into 50–70 ml of fresh medium. During the month before experiments clones were reinoculated every 5–7 days to induce exponential growth. In experiments, the clones were transferred into 50 mm diameter glass Petri dishes (bottom area 494 $mm^2$) with the following salinity gradients: 8, 12, 18, 24, 30, 36, 42, 48, 54, 60‰ (Black Sea and New Zealand clones) and 14, 18, 24, 30, 36, 42, 48, 54, 64‰ (Tenerife clones). Salinity adjustments were made by either diluting ESAW medium with distilled water, or adding sodium chloride. The number of cells was counted in ten fields of view (0.88 $mm^2$ each) of Nib-100 inverted microscope at 20× lens and 10× eyepiece magnification within four days. The specific growth rate (r) was calculated from cell counts using the model of exponential growth (Wood *et al.,* 2005):

$$N_t = N_0 e^{rt}$$

where $N_0$ is cell number at the beginning of the experiment, $N_t$ is cell number at the end of the time interval, and r is a specific growth rate calculated by the least squares method (MS Excel). The growth rate r was converted to doubling per day (k) by dividing r by the natural log of 2.0.

To determine the optimal salinity for growth, data were approximated by a second-order polynomial equation and then the first derivative was calculated and set to zero to find maximum. Experiments were fulfilled in duplicates, with two different clones from each population.

**Microscopy**: Two strains, 5.0630-F (*Climaconeis aucklandensis* sp. nov.) and 8.0305-A (*C. scalaris*), maintained in the stationary growth phase were used for laser scanning microscopy (LSM). Cells were fixed with 4% paraformaldehyde solution in PBS (0.1 M, pH 7.4) for 30 minutes, washed with PBS three times and stained with DAPI (10 µg/ml). The cells were then embedded in mounting media Mowiol® 4-88 (Merck KGaA, Germany) and examined using a laser scanning microscope LSM 710 (Zeiss, Germany).

Chloroplast autofluorescence was excited with a 561 nm laser and its emission registered in the range of 650–723 nm. DAPI fluorescence was excited with a 405 nm laser and its emission was registered in the range of 415–512 nm. 3D-reconstruction was obtained from 150–300 optical sections (thickness on the z axis: 0.043–0.118 µm). For each species, at least 10 chloroplasts from different cells were reconstructed. The images were minimally processed in ZEN 2010 software: shown in transparent mode with the maximum channel threshold for noise elimination of 10 units.

For transmission electron microscopy (TEM), cells were fixed with 2.5% glutaraldehyde and 1% paraformaldehyde in culture medium for 1 hour and then with 2.5% glutaraldehyde and 2% paraformaldehyde in PBS (0.1 M, pH 7.4) with the addition of tannic acid (final concentration 0.5%) for 2.5 hours. After washing in PBS cells were postfixed with 1% osmium tetroxide solution for 16 hours. After this, cells were washed three times in PSB and embedded in 1% agar. Further dehydration and resin embedding were performed as describe earlier (Bedoshvili & Likhoshway, 2012). Sections were obtained with a Diatome diamond knife (Germany) and stained with uranyl acetate and lead citrate. Preparations were examined with a Zeiss Leo 906 E transmission electron microscope (Carl Zeiss, Germany) at an acceleration voltage of 80 kV. Micrographs were taken with a Zeiss MegaView II camera. Measurements were performed on 10 sections from different cells (3 measurements per sections) with Zeiss Mega View II software.

The names of taxa of higher rank are according to Round *et al.* (1990) and Cox (2015). Terminology follows Davidovich (2017), Gogorev *et al.* (2018, 2024), and the special term "additional slit" is taken from Lobban *et al.* (2010).

## Results

### Life form

Vegetative cells of *Climaconeis aucklandensis sp. nov*., like those of *C. scalaris*, are predominantly solitary and randomly dispersed on the bottom of Petri dishes due to active gliding. Occasionally, cells formed loose chains (Figure 1), where they were not physically connected but glided freely along a shared mucilage track, occasionally contacting one another. When encountering obstacles, cells either stopped or reversed direction but remained adherent to the mucilage track, never deviating from it. This behavior resembles that of certain motile

diatoms, such as some species in the genus *Berkeleya* Greville, which produce not only mucilage tracks but also mucilage tubes.

In laboratory cultures, the cell length of *C. aucklandensis* sp. nov. ranged from 104 µm (initial observations) to 31 µm (final measurements). However, this range likely underestimates natural variability, as the studied clones did not include larger cells resulting from sexual reproduction. In contrast, *C. scalaris* displayed a broader size range, with apical cell length varying from 228 µm (initial and post-initial cells) to 24 µm (smallest observed cells), representing a 9-fold decrease in size.

Live cells of *C. aucklandensis* sp. nov. contained multiple H-shaped chloroplasts (Figure 2, 3), with their numbers per cell ranging from 4 in the smallest cells (at the end of the life history) up to 12 in the largest observed (but not initial or postinitial) cells. However, the full size range of this species remains undetermined, as the length of initial cells is currently unknown. For comparison, in *C. scalaris*, a species with a better-studied size range, the number of chloroplasts per cell varied from 3 to 18 (Figure 4, 5).

**Chloroplast ultrastructure**

Laser scanning microscopy (Figures 6–13) was performed on *Climaconeis scalaris* clone 8.0305-A, which contained 9–12 chloroplasts (Figure 6, 7), and on *C. aucklandensis* sp. nov. clone 5.0630-F, which showed 7–8 chloroplasts per cell (Figure 10, 11). In both species, the chloroplasts exhibited an H-shaped morphology, with two lobes adhering to the frustule near the girdle bands and a central bridge (Figure 8, 12). The nuclei were rounded to slightly elongated and located in the cell center. Optical sections revealed non-fluorescent pyrenoid regions and chloroplast stroma with sparse pigment distribution (Figure 9, 13).

Transmission electron microscopy (Figures 14–21) revealed that all chloroplasts of both species possess clearly visible girdle lamellae (Figure 14, 18). In *C. scalaris*, pyrenoids appeared either triangular (Figure 14, 15, 17) or slightly rounded (Figure 16), with their periphery often penetrated by one or two transpyrenoid lamellae, each consisting of two thylakoids. In *C. aucklandensis*, pyrenoids exhibited bean-shaped or obtusely triangular forms (Figure 18), with one or two transpyrenoid lamellae arranged in a complex manner near the pyrenoid center (Figure 18, 20).

The periplastidial compartments in both species were poorly developed and rarely observed in sections (Figure 14, 15, 19, 21). As in most diatoms, thylakoids lacked grana and were strictly organized into stacks of three (Figure 16, 19). In *C. aucklandensis* sp. nov. thylakoids were packed more tightly than in *C. scalaris*. Measurements indicated that thylakoid stacks in *C. aucklandensis* had a thickness of 56.3±6.0 nm, while those in *C. scalaris* measured 53.2±6.9 nm. The distance between stacks varied, averaging 33.4±4.8 nm for *C. aucklandensis* and 48.9±15.6 nm for *C. scalaris*.

**Taxonomy**

To reflect the principal morphological disparity within the genus *Climaconeis* and to facilitate its future taxonomic revision, we propose a provisional framework of three sections. This classification is based on a combination of two key morphological characters: valve shape (straight *vs.* curved) and the presence or absence of craticular bars on the valvocopula. While these represent the most prominent and consistent macro-morphological features available for the genus to date, it is critical to emphasize that this system is a morphological hypothesis. Its primary aim is to structure current knowledge and generate testable predictions for future phylogenetic studies, as the available molecular dataset is currently too sparse and biased to robustly evaluate the monophyly of these groups. The proposed sections are as follows:

**Division Bacillariophyta**

Class Bacillariophyceae Haeckel emend. Medlin *et* Kaczmarska

Order Naviculales Bessey

Family Berkeleyaceae D.G. Mann

Genus *Climaconeis* Grunow emend. E.J. Cox

Section *Climaconeis*

Type species *Climaconeis lorenzii* Grunow 1862, Verhandlungen der kaiserlich-königlichen zoologisch-botanischen Gesellschaft in Wien, 12: 421, pl. 8: Figure 7.

Description: valves straight, valvocopulae with craticular bars (*scalariform valvocopula*).

*Climaconeis coxiae* G.Reid *et* D.M.Williams 2002

*Climaconeis lorenzii* Grunow 1862

*Climaconeis oculata* (J.Brun) Kuntze 1898 (Note: The historical taxon *C. oculata* (J.Brun) Kuntze 1898 was also described with structures resembling craticular bars, but its identity remains dubious)

*Climaconeis stromatolitis* J.John 1991

Section *Lineatae* Gogorev *sect. nov*.

Type species *Climaconeis scalaris* (Brébisson) E.J.Cox 1982, British Phycological Journal, 17: 166.

Description: valves straight, valvocopulae without craticular bars.

*Climaconeis aucklandensis sp. nov*.

*Climaconeis colemaniae* A.K.S.K.Prasad 2010

*Climaconeis delicatula* (Cleve) E.J.Cox 1982

*Climaconeis fasciculata* (Grunow *ex* Cleve) E.J.Cox 1982

*Climaconeis mabikii* J.Park, Khim *et* J.H.Lee 2016

*Climaconeis minaegensis* Lobban 2021

*Climaconeis petersonii* Lobban, Ashworth *et* Theriot 2010

*Climaconeis scalaris* (Brébisson) E.J.Cox 1982

*Climaconeis scopulorioides* (Hustedt) E.J.Cox 1982

*Climaconeis undulata* (Meister) Lobban, Ashworth *et* Theriot 2010

Section *Curvatae* Gogorev *sect. nov.*

Type species *Climaconeis inflexa* (Brébisson ex Kützing) E.J.Cox 1982, British Phycological Journal, 17: 166.

Description: valves curvate, valvocopulae without craticular bars.

*Climaconeis desportesiae* Lobban 2018

*Fottea, 26*(2), 140–155, 2026
doi: 10.5507/fot.2026.001

*Climaconeis ghurbensis* G.Reid *et* D.M.Williams 2002
*Climaconeis guamensis* Lobban, Ashworth *et* Theriot 2010
*Climaconeis inflexa* (Brébisson *ex* Kützing) E.J.Cox 1982
*Climaconeis koenigii* A.K.S.K.Prasad 2000
*Climaconeis leandrei* Lobban 2018
*Climaconeis riddleae* A.K.S.K.Prasad 2003
*Climaconeis silvae* A.K.S.K.Prasad 2003
*Climaconeis tarangensis* Lobban 2021

Section Lineatae includes the newly described species:

***Climaconeis aucklandensis* Gogorev, O.Davidovich *et* N.Davidovich *sp. nov*. (Figures 1–3, 22, Supplementary Plates I–III)**

≡ *Climaconeis* sp. in Gastineau *et al.* 2021, Int. J. Mol. Sci., 22: 3, Figure 1C.

**Description**

**LM** (Figures 1–3, 22, Supplementary Plate I): Cells straight, rarely undulate, usually solitary, but sometimes tend to grow in rows. Chloroplasts H-shaped, 4 to 12 pairs. Valves linear, 31–104 µm long, 5.0–10.4 µm wide, with slight inflated middle and rounded to slightly capitate apices. Valve mantle low. Axial area narrow, lanceolate. Central area small, rounded to elliptical.

**SEM** (Figures 23–30, Supplementary Plates II–III): Raphe straight, central endings close one to other, about distance of 4 striae, no stauros. Inside axial area raised with raphe branches in small depression, terminal endings consist small helictoglossa. Striae parallel, slightly radial near center (Figure 28), weakly convergent to the ends, usually shorter and indistinct at center, uniseriate, 15–19 (up to 22 near apices) in 10 µm, composed of small areolae, 2–3 in 1 µm, rounded to rounded-square and apically elongated to slit-like near margin. One row of slit-like areolae on valve mantle margin, including apex area (Supplementary Plate II, 1, 2). Inside foramen of one row of areolae in one side near raphe located practically perpendicular to valve face and foramen of other areolae, so external openings of these areolae are slit-like and generally connected in "additional slit" (term from Lobban *et al.,* 2010), as a continuous or dotted line (Fig 28, Supplementary Plate II, 1, 2). Girdle bands open, very shallow, 2–8.5 µm high, with 1–2 rows of rounded or oblong poroids, 2–3 in 1 µm; valvocopulae open or closed, with dentate margin, without craticular bars, also with 2 rows of smaller poroids, sometimes connected as slit, rarely there is third row of more dense poroids on advalvar margin, 6.0–6.5 in 1 µm (Supplementary Plate III, 1–8).

The new species is morphologically similar to *Climaconeis undulata* in frustule appearance and chloroplast number, and to *C. fasciculata* in general morphology. While the ranges of valve length, width, stria density, and chloroplast number overlap between *C. aucklandensis sp. nov*., *C. undulata,* and *C. fasciculata*, the lower limits of valve length, width, and stria density in *C. aucklandensis sp. nov*. exceed those of the latter two species. It differs from *C. scalaris* primarily by its lower stria density (for detailed comparison, see Table 2).

**Holotype:** Slide no. LE A0004260 (strain 5.0630-OF), kept in the Algological Herbarium of the Komarov Botanical Institute (LE), St. Petersburg, Russia. The holotype specimen is illustrated in Figure 22.
**Isotypes:** Slides no. LE A0004255 – A0004259, A0004261, kept in Algological Herbarium of the Komarov Botanical Institute (LE), St. Petersburg, Russia.
**Type locality:** New Zealand, North Island, Auckland, Viaduct Basin, coordinates 36°50'28.32"S, 174°45'33.39"E, 20 May 2015, leg. Andrzej Witkowski.
**Habitat:** marine perithyton.
**Etymology:** The epithet refers to the geographic location of the species.
**Distribution:** Marine benthic notal species, recorded only in *locus classicus*.
**Gene sequence:** plastid-encoded *rbc*L gene sequence data were deposited in the GenBank under accession numbers: PV262172 (5.0630-OC), PV262173 (5.0630-OD), PV262174 (5.0703-OB), and PV262175 (5.0703-OK).
**Reference strains:** 5.0630-OB, 5.0630-OC, 5.0630-OD, 5.0630-OF, 15.0703-OK maintained in the World Ocean Diatom Collection (WODC) at the Karadag biological station, Crimea.

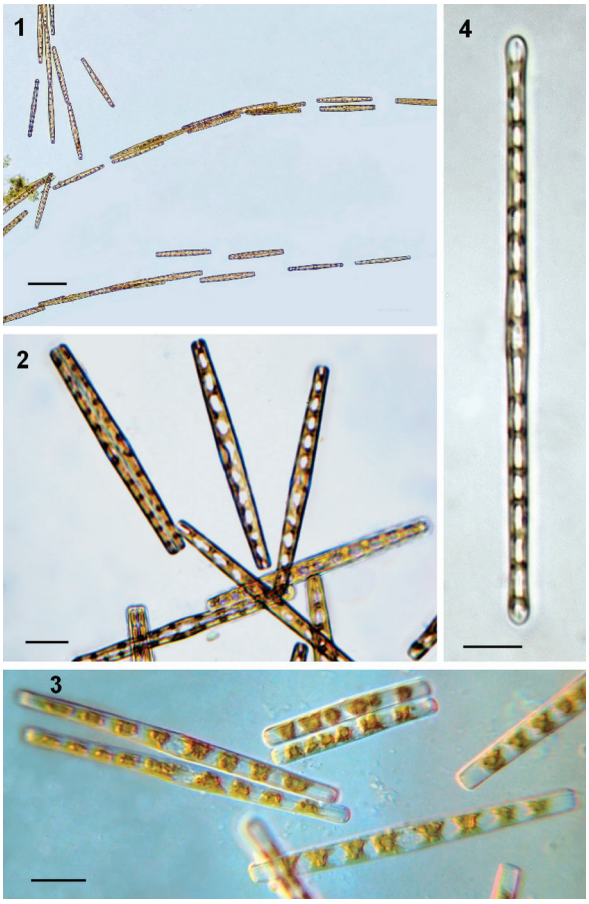


**Figures 1–4**. Live cells of **(1–3)** *Climaconeis aucklandensis sp. nov*. and (4) *C. scalaris.* **(1)** Cultured cells, typically solitary but occasionally forming linear arrangements. **(2)** H-shaped chloroplasts. **(3)** Chloroplast number correlating with apical cell length. **(4)** The longest cells had the maximum chloroplast count (17–18). Scale bars 50 µm (1), 20 µm (2–4).

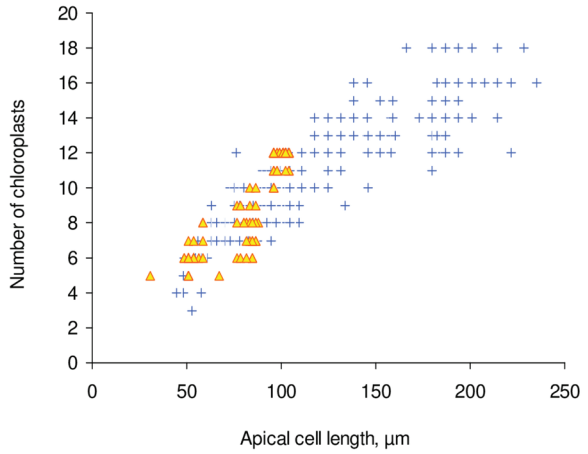


**Figure 5**. Relationship between apical cell length and chloroplast number per cell in *Climaconeis aucklandensis* sp. nov. (triangles) and *C. scalaris* (Black Sea population; crosses).

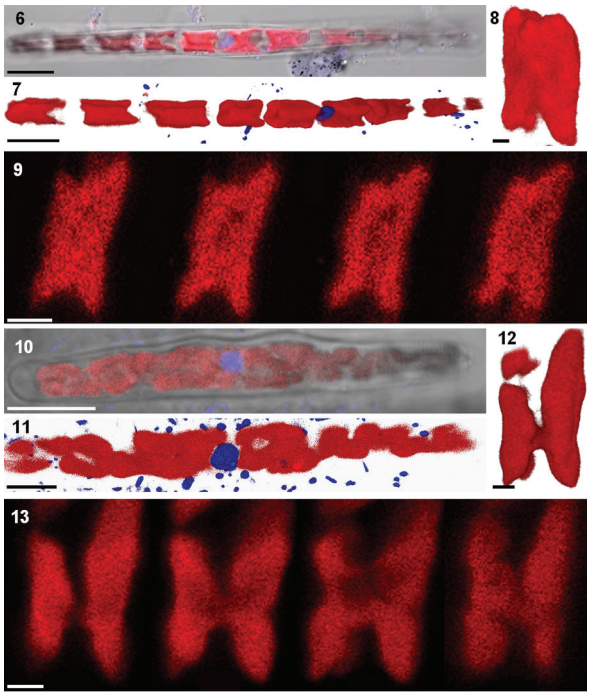


**Figures 6–13**. Chloroplasts in cells of **(6–9)** *Climaconeis scalaris* and **(10–13)** *C. aucklandensis sp. nov*., imaged by laser scanning microscopy (LSM). **(6, 10)** single optical section showing a cell in phase contrast merged with chloroplast autofluorescence and DAPI staining. **(7, 11)** 3D-reconstruction of chloroplast autofluorescence and the DAPI stained nucleus. **(8, 12)** 3D-reconstruction of autofluorescence for a single chloroplast; serial optical sections of chloroplasts for **(9)** *C. scalaris* (section thickness 0.043 µm) and for **(13)** *C. aucklandensis* (section thickness 0.118 µm). Chloroplast autofluorescence is shown in red and DAPI staining in blue. Scale bars 10 µm (6, 7, 10, 11), 1 µm (8, 12), 2 µm (9, 13).

Morphological and biometric characteristics of *Climaconeis scalaris* specimens from the Black and Mediterranean seas (Supplementary Plates IV–VII) generally corresponded to data by Davidovich *et al.* (2019) and are more extensive than the original description by Cox (1982), especially in chloroplast number and valve length (for details see Table 2).

Cells solitary, with H-shaped chloroplasts in pairs. Valves linear-lanceolate, with slight inflated middle and rounded to slightly capitate apices. Valve mantle low. Axial area narrow, lanceolate. Striae parallel, uniseriate, usually 1–3 striae shorter and indistinct at center. Striae composed of rounded to rectangular elongated areolae, 2.5–3.0 in 1 µm. Sometimes one row of areolae located near raphe with slit-like external openings and generally connected in "additional slit". The regular valve structure continues with interruption to the apex. Inside valve face practically closed by broad, perhaps T-formed ribs, except apical zones with apical pore field. Girdle bands open, very shallow, 0.7–1.5 µm high, with 1–2 rows of rounded poroids, 24–30 in 10 µm. Valvocopulae open or closed, with weakly dentate/undulate margin.

Slides no. LE A0004263 – A0004267 with specimens of *C. scalaris* are kept in Algological Herbarium of the Komarov Botanical Institute (LE), St. Petersburg, Russia. Reference strains 5.0720-OD, 5.0720-OZ, 5.0807-OC, 5.0812-OA, 9.0920-OD, 22.0809-OA, 23.0820-OE, and 23.0820-OB are maintained in culture in WODC. *rbc*L gene sequences obtained from isolated strains of *C. scalaris* were deposited in GenBank under accession numbers: PV262178 (8.0118-OA), PV262179 (23.0820-OA), PV262180 (23.0820-OB), PV262181 (23.0820-OD), PV262182 (23.0820-OE).

Strains of *Climaconeis* cf. *scalaris* had morphological and biometric characteristics (Supplementary Plates VIII–X) similar to those of *C. scalaris*. Slide no. LE A0004262 with *Climaconeis* cf. *scalaris* kept in Algological Herbarium of the Komarov Botanical Institute (LE), St. Petersburg, Russia. Reference strains 8.0601-OA and 8.0601-OB are maintained in WODC. Their gene sequences were deposited in GenBank under accession numbers: PV262176 (8.0601-OA) and PV262177 (8.0601-OB).

### Relation to salinity

The dependence of growth rate on salinity was well described by a parabolic model (Figure 31). Tolerance limits are relatively broad, spanning from approximately 4 to 56‰ in clones of *Climaconeis* from the Black Sea, and from 14 to 60‰ in clones from Auckland. The investigated clones exhibited distinct salinity optima: 29.9‰ for Black Sea clones, 33.8‰ for Atlantic clones, and 37.9‰ for New Zealand clones. The optimal salinity levels of oceanic populations closely matched the typical salinities of their natural habitats. In contrast, the optimum for Crimean clones was significantly higher than the ambient salinity of their Black Sea sampling sites (17–18‰).

### Molecular analysis

The *rbc*L gene sequence divergence among available *Climaconeis* species varied from 2.58 to 9.78% (Table 3). The sequences of the new species differed from

*Fottea, 26*(2), 140–155, 2026
doi: 10.5507/fot.2026.001

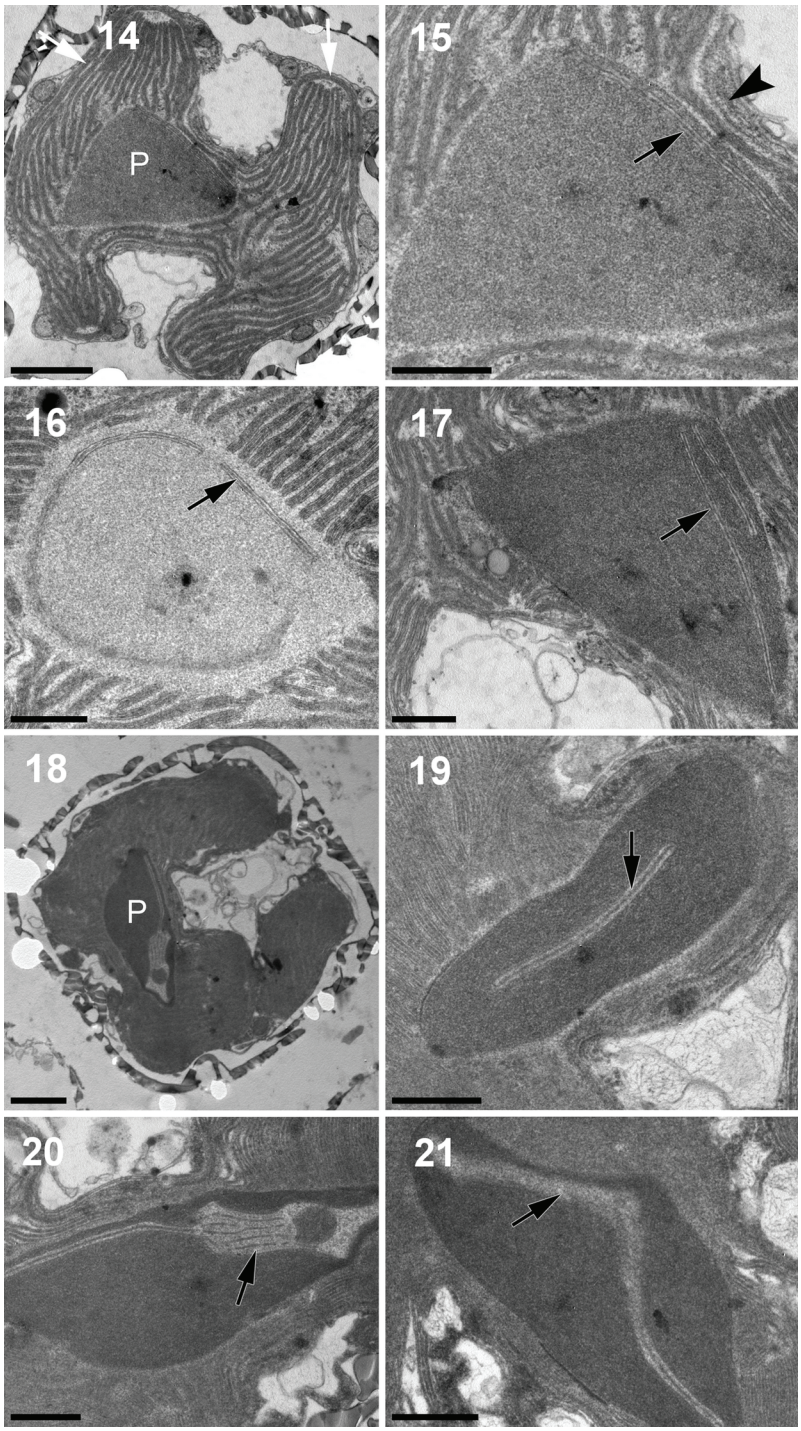


**Figures 14–21**. Chloroplast ultrastructure of **(14–17**) *Climaconeis scalaris* and **(18–21)** *C. aucklandensis sp. nov*., imaging by transmission electron microscopy (TEM): triangular pyrenoids on the cell sections of **(15, 17)** *C. scalaris* and **(18, 20, 21)** *C. aucklandensis*; apparently slightly rounded **(16)** and lenticular **(18)** pyrenoids are extreme forms of triangle. Black arrows – transpyrenoid lamella; white arrows – girdle lamella; black arrowheads – periplastidial compartment; white arrowhead – thylakoid stacks. Scale bars 1 μm (14, 18), 500 nm (15–17, 19–21).

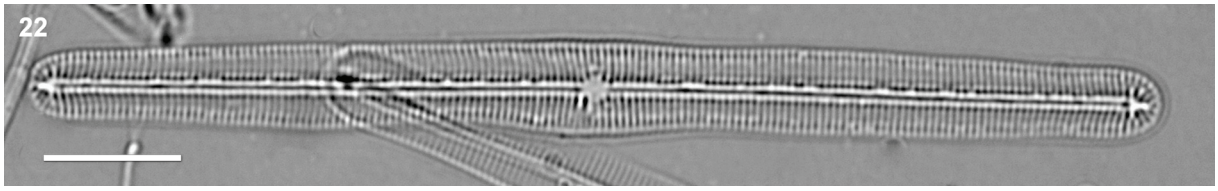


**Figure 22**. The holotype specimen of *Climaconeis aucklandensis* Gogorev, O.Davidovich et N.Davidovich *sp. nov.* Slide no. LE A0004260 (strain 5.0630-OF); kept in the Algological Herbarium of the Komarov Botanical Institute (LE), St. Petersburg, Russia.

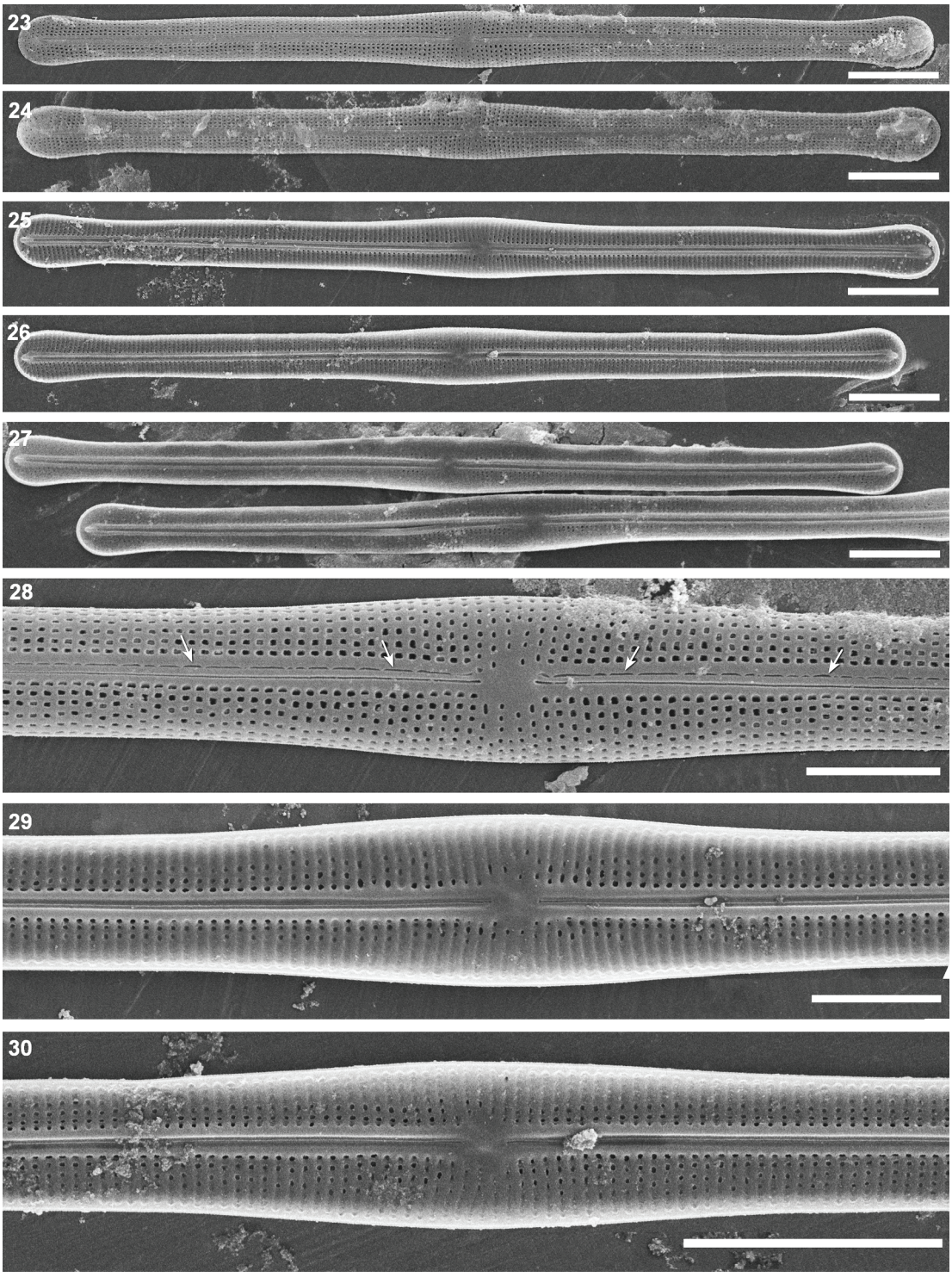


Figures 23–30. *Climaconeis aucklandensis sp. nov*., valves. **(23, 24)** External view. **(25–27)** Internal view. **(28)** Middle part, exterior, dotted "additional slit" (arrows). **(29, 30)** interior. Scanning electron microscopy (SEM). Scale bars 10 µm (23–27, 30), 5 µm (28, 29).

other species by more than 4.45%, while intraspecific difference was very low (0–0.04%). The results suggested that we were likely dealing with a new species. To test this hypothesis, we determined the phylogenetic position of our clones using a dataset of 17 *Climaconeis* accessions (Figure 32). Phylogenetic analyses placed the new clones into three distinct lineages. The sequences of the New Zealand clones were identical and formed a separate clade, with *Climaconeis* cf. *lorenzii* (Saudi Arabia, Corniche area, Jeddah) as a sister taxon. The second lineage comprised identical sequences of Canary Island clones, which showed high statistical support (100/1.00), was sister to the second and included sequences from Turkey and the Black Sea. The basal position in the genus tree was occupied by single sequences of *C. undulata* (USA, Talofofo Bay, Guam) and *C. riddleae*

**Table 2.** Comparison of morphologically similar *Climaconeis* species.

| *Climaconeis species* | Plastids (in pairs) | Length (µm) | Width (µm) | Striae in 10 µm | Geography | Locations | References |
|---|---|---|---|---|---|---|---|
| *Climaconeis aucklandensis sp. nov*. (N = 281) | 4–12 | 31–104 | 5.0–10.4 | 15–19(22) | notal | New Zealand | This study |
| *C. undulata* | – | 86 | 8 | 20 | tropical | China (Amoy Bay) | Meister, 1932[1] |
| | 7–13 | 99–117 | 7–9 (6–7 apex) | 18–20[1] | tropical | China, Sumatra, Guam | Lobban *et al.,* 2010 |
| *C. fasciculata* | 10 | 72 | 6–7 | | | California | Merezhkovsky, 1901 |
| | | 64–120 | 12 | 20–24 | tropical | Bengal | Hustedt, 1961 |
| | | 90–120 | 10–12[2] | 17–19 | | | Cox, 1982 |
| *C. scalaris* | 8–19 | | | | temperate | Black Sea | Merezhkovsky, 1901 |
| | 8–10 | 68–86 | 5.5–8 | 20 | | Europe (France) | Cox, 1982 |
| | 7–13 | 71–150 | 6–9 | 18 | | Guam | Lobban *et al.,* 2010 |
| | 10–12 | 88–91 | 5.5–6.3 | 21 | | | Lobban, 2018 |
| | 3–18 | 29–229 | 6.4–8 | 20 | | Black Sea | Davidovich *et al.,* 2019 |
| (N = 788) | 3–18 | 24–228 | 4.8–5.6 | 18–19 | | Black Sea | This study |
| (N = 90) | 4–10 | 47–128 | 4.8–6.4 | 18–21 | subtropical | Mediterranean Sea | This study |
| *Climaconeis* cf. *scalaris* (N = 187) | 4–10 | 36–120 | 4.8–12.7 | 19–21 | tropical | Canary Islands | This study |
| *C. coxiae* | 10–13 | 110–130 | 5–6 | 16 | tropical | Abu Dhabi, Mexico, Guam | Reid & Williams, 2002 |
| *C. inflexa* (Brébisson *ex* Kützing) E.J. Cox | 2 | 80–220 | 7–11 | 19–23 | temperate | Europe[3] (Calvados), New Zealand, S.Africa | Cox, 1982 |
| | 2 | 100 | 5–8 | 18 | | Guam | Lobban *et al.,* 2010 |
| *C. silvae* | 4–10 (8–20[3]) | 132–298 | 5–10 | 28–35 | tropical | Florida[3], Puerto Rico | Prasad, 2003 |
| | 12–18 | 190–210 | 7–10 | 28–30 | | Guam, Palau | Lobban *et al.,* 2010 |

Note: [1)] as *Gomphocaloneis undulata*; [2)] Cox, 1982; [3)] Lobban, 2018.

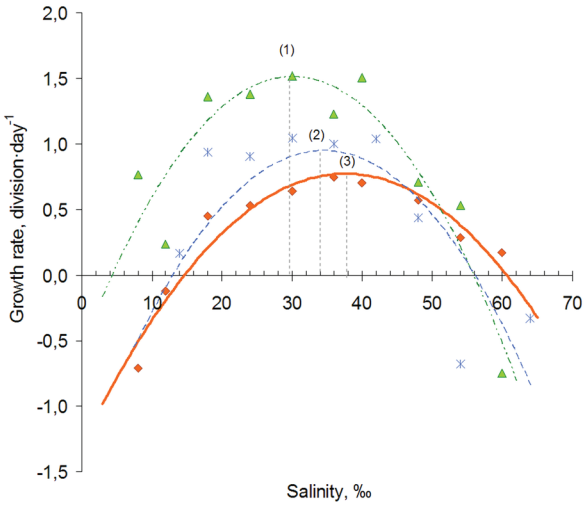


**Figure 31**. Growth rate dependence on salinity in *Climaconeis* clones from three geographically distant populations. **(1)** Black Sea, Crimean Peninsula (optimum 29.9‰). **(2)** Tenerife, Canary Islands (optimum 33.8‰). **(3)** Auckland, New Zealand (optimum 37.9‰). The data are fitted with a parabolic function.

(USA, Umatac Bay, Guam).

Three molecular species delimitation methods (ASAP, PTP, and GMYC) consistently identified six species-level clusters. The new species clones, the Canary Islands lineage, and the Turkey–Black Sea lineage each represented separate clusters.

### Sexual compatibility

Mating experiments were performed in pairwise combinations of clones from the Black Sea and the Mediterranean Sea. Three Black Sea clones were found to be of the same mating type and showed vigorous mating with three Mediterranean Sea clones of the opposite mating type (Table 4). Clone 23.0820-OB from the Mediterranean Sea exhibited rare intraclonal reproduction.

## Discussion

### Taxonomy and morphology

The morphological diversity observed within *Climaconeis* led us to propose a sectional classification, providing a framework for the genus based on two prominent and easily observable characters: valve shape and the presence of craticular bars. According to this system, species are primarily divided into two groups based on valve shape: those with straight (linear to linear-lanceolate) valves and those with curved (lunate) valves. The linear-valved group is further subdivided by the presence or absence of craticular bars on the valvocopula—a significant morphological feature that, as Cox (1982, p. 165) suggested, "could have precipitated a change to numerous chloroplasts". This latter feature also shows similarity between linear-valved *Climaconeis* species and the genera *Climacosphenia* Ehrenberg and *Diatomella* Greville.

Based on these two characters, we propose three new sections within *Climaconeis*: *Climaconeis, Lineatae,* and *Curvatae*. However, it is important to note that valve curvature, while a useful diagnostic character, is known to be a homoplastic trait in other raphid diatom genera. Therefore, these sections should be interpreted as formalized morphological groups that structure the current knowledge of the genus and generate testable hypotheses for future phylogenetic studies, rather than as confirmed phylogenetic clades.

The recently described *Climaconeis heteropolaris* C. Radhakrishnan, V. Gokul, Anish, Kociolek *et* B. Karthick (Cheran *et al.*, 2025) disrupts all our coherent discussions of three sections within the genus. It differs from all previously described species in its heteropolarity of valves and the presence of stauros and internal periraphic ribs (as in the genus *Frustulia*). Deciding which section to assign it to is beyond the scope of our article.

The section *Climaconeis* comprises four species, including *Climaconeis oculata*. Brun (1894) originally described *Lamella oculata*—a taxon not subsequently recorded in the available literature—and noted in the protologue the presence of distinct internal nodes ("rudiments de fausses cloisons?") and "demarcation lines" on the internal valve surface. These lines extend longitudinally adjacent to the nodes and exhibit fine striation similar to that of the valve. Therefore, we can confidently infer that these nodes and lines are outgrowths or septa of the valvocopula. Based on these structures, Brun (1894) noted the similarity between this new species and both the genus *Climacosphenia* and the only known species of *Climaconeis* at that time, *C. lorenzii*.

Despite its clear genetic distinctness, *Climaconeis aucklandensis* sp. nov. exhibits a striking morphological similarity to *C. scalaris* and *Climaconeis* cf. *scalaris*, underscoring the potential for cryptic diversity within this group. This similarity is particularly intriguing in light of the significant genetic differences between these taxa. The most reliable diagnostic feature to separate them is the markedly lower stria density in *C. aucklandensis sp. nov.*, as valve dimensions and chloroplast number show overlapping ranges (see Table 2). A detailed pairwise comparison with *C. scalaris* further reveals differences in several morphological traits: (1) chloroplast number is generally higher in *C. scalaris*; (2) the range of valve length is broader in *C. scalaris*; and (3) the range of valve width is broader in *C. aucklandensis*. It is noteworthy that literature reports for *C. scalaris* document even larger valve widths (Cox, 1982; Davidovich *et al.,* 2019; Lobban *et al.,* 2010) than those observed in our material. Nevertheless, the most consistent and significant diagnostic difference remains the stria density, which is markedly higher in *C. scalaris*.

The comparison of *Climaconeis* cf. *scalaris* and *C. scalaris* reveals a greater range in both chloroplast number and valve length in *C. scalaris*. These species differ primarily in valve width (broader in *Climaconeis*

*Fottea, 26*(2), 140–155, 2026
doi: 10.5507/fot.2026.001

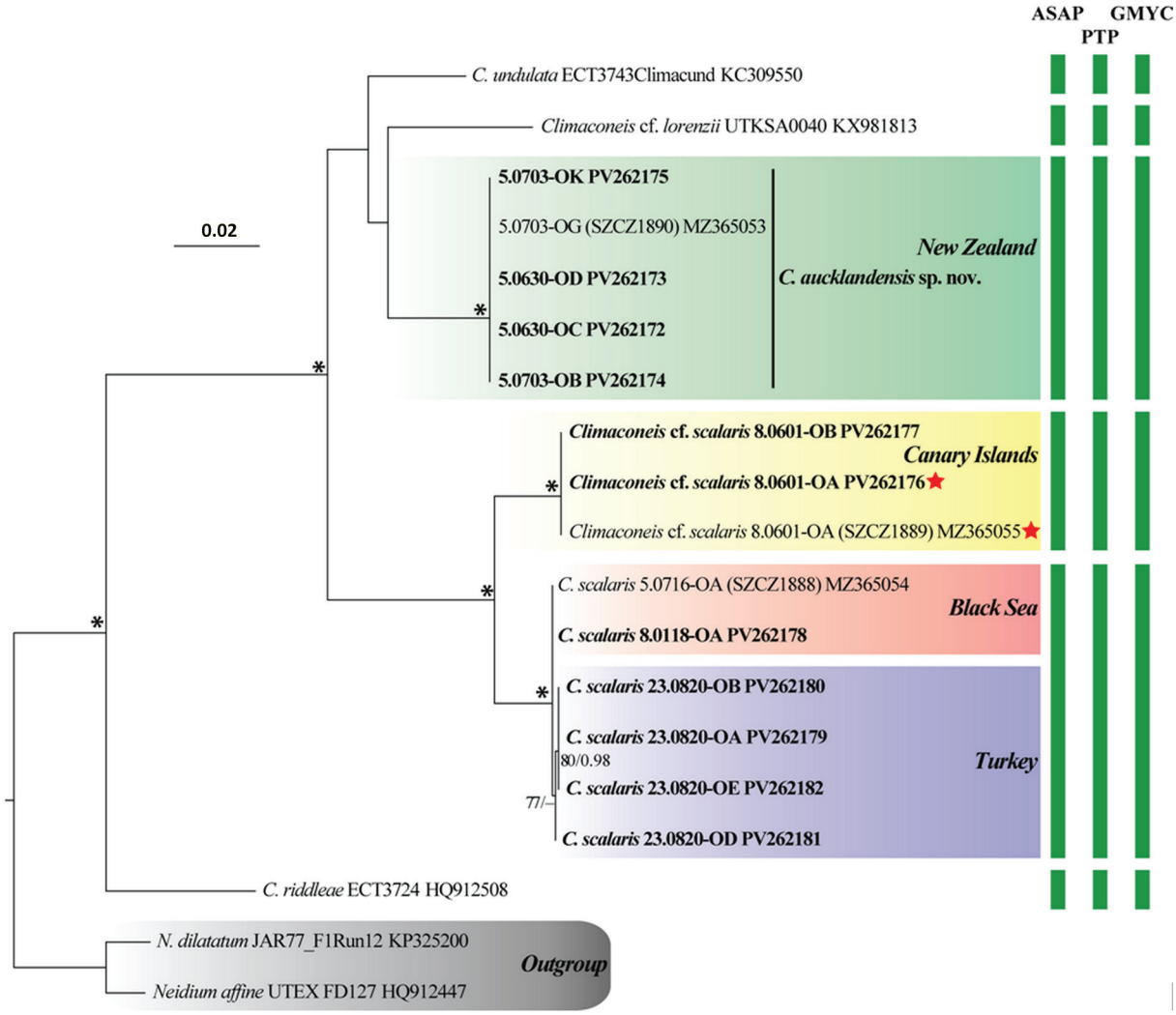


**Figure 32**. Maximum likelihood (ML) tree illustrating the phylogenetic position of *Climaconeis* species, based on plastid-encoded *rbc*L gene sequence (GTR+I model). Support values [ML/BI, BP ≥ 70% and PP ≥ 0.95] are shown below the branches. Newly sequenced clones are highlighted in bold. Nodes with full support (100% BP and 1.00 PP) are marked by an asterisk. Stars denote clones with identical sequences, derived from the same culture after a three-year interval. Rectangles indicate species-level clusters identified by the ASAP, PTP, and GMYC species delimitation methods. Scale bar represents substitutions per nucleotide site.

cf. *scalaris*) and areolae density (higher in *Climaconeis* cf. *scalaris*). Notably, the Black Sea population of *C. scalaris* exhibits lower stria density compared to the Mediterranean population.

Lobban *et al.* (2010, p. 298, Figures 23, 25) introduced the term "additional slit" for *Climaconeis undulata*. Our analysis of literature and original data reveals that this morphological feature occurs not only in *C. undulata* but also in the new species *C. aucklandensis*, *C. mabikii* (Park *et al.,* 2016, Figure 3b–d), and *C. scalaris* (e.g. see the Black Sea population, Supplementary Plate VI, 3; VII, 1). In our study, this structure was consistently observed in cultured cells, including post-initial cells formed after sexual reproduction, which indicates it is a stable species-specific trait and not a teratology.

Park *et al.* (2016) noted that *Climaconeis mabikii* resembles *C. undulata* in its slightly wavy valve outline and chloroplast number, but differs in its larger dimensions (110–185 µm long × 12–13 µm wide vs. 99–117 µm long × 7–9 µm wide) and potentially in areolae shape. In our assessment, both species share the characteristic "additional slit" adjacent to the raphe, which runs along the one side in such a way that the first row of areolae appears displaced (Figure 33). Like the stria, this dotted line is composed of modified areolae (Park *et al.,* 2016, Figures 3c, d). This shared morphological feature suggests a potential phylogenetic link between *C. mabikii*, *C. undulata*, and *C. aucklandensis*, a hypothesis that could be tested by future molecular studies.

## Chloroplasts

Although diatom taxonomy is primarily based on the morphology of siliceous frustules, apart from marker genes (Guiry & Guiry, 2025; Medlin, 2015, 2016; Theriot *et al.,* 2010), efforts have also been made to utilize chloroplast structure and pyrenoid ultrastructure for classification (Bedoshvili *et al.,* 2009; Mann, 1998; Medlin & Kaczmarska, 2004; Mereschkowsky, 1901a;

**Table 3**. Pairwise *P*-distances (%) among *Climaconeis* species/populations based on aligned *rbc*L gene sequences (1405 positions).

| № | Species | 1 | 2 | 3 | 4 | 5 | 6 | 7 |
|---|---|---|---|---|---|---|---|---|
| 1 | *C. scalaris* (Black Sea) | 0.00 | 0.09 | 0.43 | 0.83 | 0.75 | 0.69 | 0.70 |
| 2 | *C. scalaris* (Mediterranean, Turkey) | 0.12 | 0.04 | 0.44 | 0.83 | 0.74 | 0.69 | 0.71 |
| 3 | *Climaconeis* cf. *scalaris* (Canary) | 2.58 | 2.69 | 0.00 | 0.84 | 0.75 | 0.72 | 0.72 |
| 4 | *C. riddleae* | 9.60 | 9.73 | 9.78 | n/c | 0.88 | 0.93 | 0.82 |
| 5 | *C. undulata* | 6.41 | 6.34 | 6.71 | 8.55 | n/c | 0.67 | 0.62 |
| 6 | *Climaconeis* cf. *lorenzii* | 6.08 | 6.02 | 6.83 | 9.57 | 5.01 | n/c | 0.66 |
| 7 | *C. aucklandensis* sp. nov. | 6.70 | 6.82 | 7.04 | 9.46 | 4.45 | 5.01 | 0.00 |

Note: Intraspecific *p*-distance values are indicated along the diagonal. Standard error estimates are shown above the diagonal. n/c – not calculated for species with one sequence.

**Table 4.** Reproductive compatibility matrix of *Climaconeis scalaris* clones derived from the Black and Mediterranean seas.

| Population location | Clone | 22.0927-OA | 22.0606-OA | 22.0606-OB | 23.0820-OB | 23.0820-OD | 22.0820-OE |
|---|---|---|---|---|---|---|---|
| Black Sea, Crimea | 22.0927-OA | | | | | | |
| Black Sea, Crimea | 24.0606-OA | 0 | | | | | |
| Black Sea, Crimea | 24.0606-OB | 0 | 0 | | | | |
| Mediterranean Sea | 23.0820-OB | **3** | **3** | **3** | [1] | | |
| Mediterranean Sea | 23.0820-OD | **3** | **2** | **2** | 0 | | |
| Mediterranean Sea | 23.0820-OE | **2** | **2** | **2** | 0 | 0 | |

Note. Sexual reproduction abundance: 3 (abundant), 2 (moderate), 1 (weak), 0 (none). Square brackets denote intraclonal reproduction. The dashed line indicates the scope of sexual compatibility.

Schmid, 2001). However, linking chloroplast or pyrenoid fine structure to diatom taxonomy remains problematic, both due to insufficient data for many species and the inherent variability of chloroplasts. Their shape, along with the arrangement of stromal membranes and pyrenoid morphology, may vary depending on the cell cycle stage and probably cultivation conditions. Consequently, it is unclear which structural features hold the greatest taxonomic significance.

While light quality is known to influence thylakoid packing in higher plants (Kirchhoff, 2013), diatoms exhibit a more rigid organization, with thylakoids typically arranged in stacks of three, sometimes displaying noticeable anastomoses (Bedoshvili *et al.,* 2009; Flori *et al.,* 2017; Pyszniak & Gibbs, 1992). Transpyrenoid lamellae have been proposed as taxonomic markers in both dinoflagellates (Dodge, 1968) and diatoms (Schmid, 2001). It is unlikely that the location of this lamella could change depending on the performance of the function of delivering carbon dioxide to Rubisco, but it could depend on the stage of the cell cycle.

The general structure of chloroplasts, including their shape and the central positioning of the pyrenoid, can clearly be considered a generic feature of *Climaconeis*. A slight difference was observed in the visualization of non-fluorescent regions: in *C. aucklandensis*, the pyrenoid regions are more pronounced, whereas in *C. scalaris*, they are nearly invisible. This discrepancy, however, might stem from better cell preservation in *C. aucklandensis* sp. nov. during fixation.

Another distinctive feature of the species could be considered the packing density of thylakoids, however, artifacts introduced by the procedure of chemical fixation and dehydration can prevent the measurement of the distance between thylakoid stacks by electron microscopy with sufficient accuracy. It is likely that the use of new techniques, such as the measurement of Bragg reflection peak in small-angle neutron scattering (Jäger & Büchel,

*Fottea, 26*(2), 140–155, 2026
doi: 10.5507/fot.2026.001

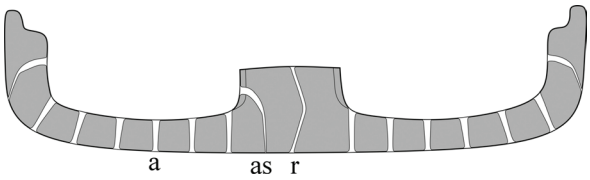


**Figure 33**. Schematic valve section of *Climaconeis aucklandensis*, illustrating the putative "additional slit". Designations: **(a)** areola; **(as)** additional slit; **(r)** raphe slit.

2019; Nagy *et al.,* 2012) could clarify this issue.

**Molecular analysis**

*Rbc*L gene sequence data are available for just 5 of the 22 currently recognized *Climaconeis* taxa (Guiry & Guiry, 2025). Increasing the taxon sampling for this marker is critical for resolving genus-level diversity.

In our study, the newly obtained *Climaconeis* sequences formed three well-supported clades: *C. aucklandensis sp. nov*. (New Zealand), *C. scalaris* (Black Sea and Mediterranean Sea), and *Climaconeis* cf. *scalaris* (Canary Islands). Breeding populations from the Black and Mediterranean Seas, considered conspecific under the biological species concept, exhibited relatively low genetic divergence (*p*-distance = 0.12). In contrast, their divergence from all other populations (except those from the Canary Islands) was significantly higher, ranging from 6.02 to 9.73%.

The Canarian population shows incipient divergence from *C. scalaris*. However, no consistent morphological traits have yet been identified to separate them. The *rbc*L sequences of the Canarian clones form a distinct, maximally supported clade, and the observed genetic divergence (2.58% from *C. scalaris* and >6.71% from other species) exceeds the interspecific threshold of delimitation in this genus (about 0.04% based on our data). Furthermore, three independent species delimitation analyses (ASAP, PTP, and GMYC) consistently recognized the Canarian lineage as a distinct species-level cluster. This molecular evidence, together with its phylogenetic distinctness, strongly suggests that the Canarian population may represent a previously unrecognized cryptic species within the genus *Climaconeis*. Further research, including mating compatibility tests and expanded morphological assessment, is required to formally evaluate its taxonomic status.

The initial phylogenetic tree presented a curious anomaly: the strain UTKSA0040, deposited as *Climaconeis* cf. *lorenzii*, was placed within the clade of section Lineatae. However, subsequent morphological analysis of this strain, conducted based on micrographs kindly provided by M. Ashworth revealed the absence of craticular bars and the presence of the 'additional slit', clearly aligning it with the section Lineatae and suggesting an affinity to *C. fasciculata* or *C. scopulorioides*. This re-assessment resolves the initial taxonomic conflict and provides independent morphological support for the molecular phylogeny, strengthening the evidence for the distinctness of the clade containing *C. aucklandensis*.

Our results highlight the hidden diversity of the genus *Climaconeis* by providing evidence for the existence of cryptic species. Morphological differentiation among the three examined strains, particularly between *Climaconeis* cf. *scalaris* 5.0716-OA (=SZCZ 1888) and 8.0601-OA (=SZCZ 1889), proves challenging using microscopy alone. Although these strains exhibit slight differences in length and width (Table 2), such variation diminishes progressively during the life cycle due to the MacDonald-Pfitzer rule.

Based solely on morphological characteristics, strains SZCZ 1888 and 1889 belong to *C. scalaris*. However, without the molecular data derived from the plastid genome, their distinction would have remained difficult. Even analysis of the nuclear small subunit ribosomal RNA gene (SSU or 18S)—a widely used barcoding marker—yielded limited resolution: the complete SSU sequences of SZCZ 1888 (MZ366484) and SZCZ 1889 (MZ366524) share 99.49% identity, with eight of nine polymorphisms localized to the first 700 bp of the 1769 bp sequence. In contrast, *rbcL* data clearly distinguished these strains (97.48% identity), revealing hidden genetic differences within morphologically similar populations (Gastineau *et al.,* 2021).

## Conclusion

Two distinct morphological characters — valve shape and the presence of craticular bars on valvocopulae — allow the division of the genus *Climaconeis* into three groups. These diagnostic features justify the recognition of three new taxonomic sections.

Populations distributed across different geographical regions (New Zealand, the Canary Islands, the Black Sea, and the eastern part of the Mediterranean Sea) reveal sufficiently high morphological similarity. Among studied strains, subtle divergence occurs in chloroplast number, valve width, and — in the Auckland population — stria density. Molecular analysis based on plastid-encoded *rbc*L gene exposed at least three divergent clades: New Zealand clones (*C. aucklandensis sp. nov*.) formed a distinct clade with maximal nodal support (100/1.0), and the Canary Islands population (*Climaconeis* cf. *scalaris*) formed a separate, well-supported clade (100/1.00), distinct from the Mediterranean and Black Sea populations. Genetic divergence among morphologically similar clones suggests cryptic speciation.

The absence of successful mating between New Zealand, Black Sea, and Canary Islands populations in cross-breeding experiments further validates their separate species status. Conversely, complete sexual compatibility between Black Sea and Mediterranean Sea strains, coupled with their genetic similarity (*p*-distance = 0.12%), confirms their classification as conspecific populations of *C. scalaris*.

**Acknowledgements**

We keep warm memories of Prof. Dr. Andrzej Witkowski, who collected and generously shared samples from New Zealand. We express our gratitude to V.N. Lishaev, L.A. Karzeva, and N. Zaporozhets for their assistance in operating the SEM. We thank Dr. Matt Ashworth (University of Texas at Austin) for kindly providing micrographs of the strain UTKSA0040. This research was conducted as a part of the State Assignment of the Ministry of Science and Higher Education of the Russian Federation, No. 124030100100-0: "Study of the Fundamental Characteristics of Marine Hydrobionts, Ensuring their Functioning in Ecosystems and Serving as the Basis for their Rational Use and Conservation". The isolation and culture maintenance of the studied strains, as well as the eco-physiological and crossing experiments, were performed by O.I. Davidovich. The morphological analysis and species description were performed by R.M. Gogorev under the institutional research project of the V.L. Komarov Botanical Institute of the Russian Academy of Sciences, No. 121021600184-6: "Flora and Taxonomy of Algae, Lichens, and Bryophytes in Russia and Phytogeographically Important Regions of the World". Transmission electron microscopy and plastid studies were conducted by Y.D. Bedoshvili using the equipment of the Shared Research Facilities for Physical and Chemical Ultramicroanalysis LIN SB RAS with the financial support of the project of the Ministry of Science and Higher Education of the Russian Federation No. FWSR-2026-0001 (1023032700153-7-1.6.17). Molecular genetic analyses were carried out by V.Yu. Nikulin and A.Yu. Nikulin under the State Assignment of the Ministry of Science and Higher Education of the Russian Federation, No. 124012400285-7. The studied strains are maintained in the Center for Collective Use "World Ocean Diatoms Collection" at the Karadag Scientific Station.

## References

Abdullin, Sh. R., Nikulin, A. Yu., Bagmet, V. B., Nikulin, V. Yu., & Gontcharov, A. A. (2021). New cyanobacterium *Aliterella vladivostokensis* sp. nov. (*Aliterellaceae*, *Chroococcidiopsidales*), isolated from temperate monsoon climate zone (Vladivostok, Russia). *Phytotaxa*, *527*(3), 221–233. https://doi.org/10.11646/phytotaxa.527.3.7

Akaike, H. (1974). A new look at the statistical model identification. *IEEE Transactions on Automatic Control*, *19*(6), 716–723. https://doi.org/10.1109/TAC.1974.1100705

Andersen, R. A., Berges, J. A., Harrison, P. J., & Watanabe, M. M. (2005). Recipes for freshwater and seawater media. In R. A. Andersen (Ed.), *Algal culturing techniques* (pp. 429–538). Elsevier Academic Press.

Bedoshvili, Y. D., & Likhoshway, Y. V. (2012). The cell ultrastructure of diatoms – Implications for phylogeny? In K. Maaz (Ed.), *The transmission electron microscope* (pp. 147–160). InTech.

Bedoshvili, Y. D., Popkova, T. P., & Likhoshway, Y. V. (2009). Chloroplast structure of diatoms of different classes. *Cell and Tissue Biology*, *3*(3), 297–310. https://doi.org/10.1134/S1990519X09030122

Bonfield, J. K., Smith, K. F., & Staden, R. (1995). A new DNA sequence assembly program. *Nucleic Acids Research*, *23*(24), 4992–4999. https://doi.org/10.1093/nar/23.24.4992

Brun, J. (1894). Espèces nouvelles. *Le Diatomiste*, *2*, 72–78.

Cheran, R., Valsan, G., Warrier, A. K., Kociolek, J. P., & Balasubramanian, K. (2025). A new species of *Climaconeis* Grunow (*Bacillariophyceae*: *Bacillariophyta*): *Climaconeis heteropolaris* sp. nov. from the southwestern coast of India. *Diatom Research*, *40*(1), 1–9. https://doi.org/10.1080/0269249X.2025.2534369

Cox, E. J. (1979). Studies on the diatom genus *Navicula* Bory. *Navicula scopulorum* Bréb. and a further comment on the genus *Berkeleya* Grev. *British Phycological Journal*, *14*(2), 161–174. https://doi.org/10.1080/00071617900650181

Cox, E. J. (1982). Taxonomic studies on the diatom genus *Navicula* Bory. IV. *Climaconeis* Grun., a genus including *Okedenia inflexa* (Breb.) Eulenst. ex De Toni and members of *Navicula* sect. *Johnsonieae* sensu Hustedt. *British Phycological Journal*, *17*(2), 147–168. https://doi.org/10.1080/00071618200650161

Cox, E. J. (2015). *Coscinodiscophyceae*, *Mediophyceae*, *Fragilariophyceae*, *Bacillariophyceae* (Diatoms). In W. Frey (Ed.), *Syllabus of Plant Families. Adolf Engler's Syllabus der Pflanzenfamilien* (13th ed., Part 2/1, pp. 64–103). Borntraeger Science Publishers.

Darriba, D., Taboada, G. L., Doallo, R., & Posada, D. (2012). jModelTest 2: More models, new heuristics and parallel computing. *Nature Methods*, *9*(8), 772. https://doi.org/10.1038/nmeth.2109

Daugbjerg, N., & Andersen, R. A. (1997). Phylogenetic analyses of the *rbcL* sequences from haptophytes and heterokont algae suggest their chloroplasts are unrelated. *Molecular Biology and Evolution*, *14*(12), 1242–1251. https://doi.org/10.1093/oxfordjournals.molbev.a025733

Davidovich, N. A. (2017). Definitions and concepts of reproductive biology of diatoms (terminological glossary). *Novosti Sistematiki Nizshikh Rastenii*, *51*, 71–105.

Davidovich, O. I., Davidovich, N. A., Gastineau, R., & Witkowski, A. (2019). Sexual reproduction of the Black Sea diatom *Climaconeis scalaris* (Brébisson) E.J. Cox. *Moscow University Biological Sciences Bulletin*, *74*(4), 200–206. https://doi.org/10.3103/S0096392519040035

Dodge, J. D. (1968). The fine structure of chloroplasts and pyrenoids in some marine dinoflagellates. *Journal of Cell Science*, *3*(1), 41–48.

Drummond, A. J., & Rambaut, A. (2007). BEAST: Bayesian evolutionary analysis by sampling trees. *BMC Evolutionary Biology*, *7*, Article 214. https://doi.org/10.1186/1471-2148-7-214

Flori, S., Jouneau, P.-H., Bailleul, B., Gallet, B., Estrozi, L. F., Moriscot, C., Bastien, O., Eicke, S., Schober, A., Bártulos, C. R., Maréchal, E., Kroth, P. G., Petroutsos, D., Zeeman, S., Breyton, C., Schoehn, G., Falconet, D., & Finazzi, G. (2017). Plastid thylakoid architecture optimizes photosynthesis in diatoms. *Nature Communications*, *8*, Article 15885. https://doi.org/10.1038/ncomms15885

Fujisawa, T., & Barraclough, T. G. (2013). Delimiting species using single-locus data and the generalized mixed Yule coalescent approach: A revised method and evaluation on simulated data sets. *Systematic Biology*, *62*(5), 707–724. https://doi.org/10.1093/sysbio/syt033

Galtier, N., Gouy, M., & Gautier, C. (1996). SEAVIEW and PHYLO_WIN: Two graphic tools for sequence alignment and molecular phylogeny. *Bioinformatics*, *12*(6), 543–548. https://doi.org/10.1093/bioinformatics/12.6.543

Gastineau, R., Davidovich, N. A., Davidovich, O. I., Lemieux, C., Turmel, M., Wróbel, R. J., & Witkowski, A. (2021). Extreme enlargement of the inverted repeat region in the plastid genomes of diatoms from the genus *Climaconeis*. *International Journal of Molecular Sciences*, *22*(13), Article 7155. https://doi.org/10.3390/ijms22137155

Gogorev, R. M., Chudaev, D. A., & Gololobova, M. A. (2024). Addition to the glossary of diatom morphology. *Novosti Sistematiki Nizshikh Rastenii*, *58*, A35–A58. https://doi.org/10.31111/nsnr/2024.58.1.A35

Gogorev, R. M., Chudaev, D. A., Stepanova, V. A., & Kulikovskiy, M. S. (2018). Russian and English

*Fottea, 26*(2), 140–155, 2026
doi: 10.5507/fot.2026.001

terminological glossary on morphology of diatoms. *Novosti Sistematiki Nizshikh Rastenii*, *52*(2), 265–309. https://doi.org/10.31111/nsnr/2018.52.2.265

Guiry, M. D., & Guiry, G. M. (2025). *AlgaeBase*. World-wide electronic publication, National University of Ireland, Galway. https://www.algaebase.org

Harper, M. A., Cassie Cooper, V., Chang, F. H., Nelson, W. A., & Broady, P. A. (2012). Phylum *Ochrophyta*: Brown and golden-brown algae, diatoms, silicoflagellates, and kin. In D. P. Gordon (Ed.), *New Zealand inventory of biodiversity: Volume 3. Kingdoms Bacteria, Protozoa, Chromista, Plantae, Fungi* (pp. 114–163). Canterbury University Press.

Hoang, D. T., Chernomor, O., von Haeseler, A., Minh, B. Q., & Vinh, L. S. (2018). UFBoot2: Improving the ultrafast bootstrap approximation. *Molecular Biology and Evolution*, *35*(2), 518–522. https://doi.org/10.1093/molbev/msx281

Hustedt, F. (1961). Die Kieselalgen Deutschlands, Österreichs und der Schweiz unter Berücksichtigung der übrigen Länder Europas sowie der angrenzenden Meeresgebiete. In L. Rabenhorst (Ed.), *Kryptogamen-Flora von Deutschland, Österreich und der Schweiz* (Band 7, pp. 1–160). Akademische Verlagsgesellschaft.

Jäger, S., & Büchel, C. (2019). Cation-dependent changes in the thylakoid membrane appression of the diatom *Thalassiosira pseudonana*. *BBA - Bioenergetics*, *1860*(1), 41–51. https://doi.org/10.1016/j.bbabio.2018.11.003

John, J. (1991). *Climaconeis stromatolitis*, a new species of diatom from Shark Bay, Western Australia. *Diatom Research*, *6*(1), 49–54. https://doi.org/10.1080/0269249X.1991.9705146

Kirchhoff, H. (2013). Architectural switches in plant thylakoid membranes. *Photosynthesis Research*, *116*(2-3), 481–487. https://doi.org/10.1007/s11120-013-9843-0

Lobban, C. S. (2018). *Climaconeis desportesiae* and *C. leandrei* (*Bacillariophyta*, *Berkeleyaceae*), two new curved species from Guam, Western Pacific. *Cryptogamie, Algologie*, *39*(3), 349–363. https://doi.org/10.7872/crya/v39.iss3.2018.349

Lobban, C. S. (2021). New species of benthic marine diatoms (*Bacillariophyta*) from the Western Pacific islands of Guam and Yap. *Phytotaxa*, *508*(3), 235–265. https://doi.org/10.11646/phytotaxa.508.3.1

Lobban, C. S., Ashworth, M. P., & Theriot, E. C. (2010). *Climaconeis* species (*Bacillariophyceae*: *Berkeleyaceae*) from western Pacific islands, including *C. petersonii* sp. nov. and *C. guamensis* sp. nov., with emphasis on the plastids. *European Journal of Phycology*, *45*(3), 293–307. https://doi.org/10.1080/09670262.2010.490924

Lobban, C. S., Schefter, M., Jordan, R. W., Arai, Y., Sasaki, A., Theriot, E. C., Ashworth, M., Ruck, E. C., & Pennesi, C. (2012). Coral-reef diatoms (*Bacillariophyta*) from Guam: New records and preliminary checklist, with emphasis on epiphytic species from farmer-fish territories. *Micronesica*, *43*(2), 237–479.

Mann, D. G. (1996). Chloroplast morphology, movements and inheritance in diatoms. In B. R. Chaudhary & S. B. Agrawal (Eds.), *Cytology, genetics and molecular biology of algae* (pp. 249–274). SPB Academic Publishing.

Medlin, L. K. (2015). A timescale for diatom evolution based on four molecular markers: Reassessment of ghost lineages and major steps defining diatom evolution. *Vie et Milieu*, *65*(4), 219–238.

Medlin, L. K. (2016). Evolution of the diatoms: Major steps in their evolution and a review of the supporting molecular and morphological evidence. *Phycologia*, *55*(1), 79–103. https://doi.org/10.2216/15-105.1

Medlin, L., & Kaczmarska, I. (2004). Evolution in diatoms. V. Morphological and cytological support of the major clades and taxonomic revision. *Phycologia*, *43*(3), 245–273. https://doi.org/10.2216/i0031-8884-43-3-245.1

Meister, F. (1932). *Kieselalgen aus Asien*. Gebrüder Borntraeger.

Mereschkowsky, C. (1901a). Etude sur l'endochrome des Diatomées. *Memoires de l'Academie Imperiale des Sciences de Saint Petersbourg, Classe Physico-Mathematique, Series 8*, *11*, 1–40.

Mereschkowsky, C. (1901b). On *Okedenia* Eul. *Annals and Magazine of Natural History, Series 7*, *8*(47), 415–423. https://doi.org/10.1080/03745480109442947

Mereschkowsky, K. S. (1903). *K morfologii diatomovyh vodoroslej* [To the morphology of diatoms]. Tipo-litografiya Imperatorskago Universiteta.

Minh, B. Q., Schmidt, H. A., Chernomor, O., Schrempf, D., Woodhams, M. D., von Haeseler, A., & Lanfear, R. (2020). IQ-TREE 2: New models and efficient methods for phylogenetic inference in the genomic era. *Molecular Biology and Evolution*, *37*(5), 1530–1534. https://doi.org/10.1093/molbev/msaa015

Nagy, G., Szabó, M., Ünnep, R., Káli, G., Miloslavina, Y., Lambrev, P. H., Zsiros, O., Porcar, L., Timmins, P., Rosta, L., & Garab, G. (2012). Modulation of the multilamellar membrane organization and of the chiral macrodomains in the diatom *Phaeodactylum tricornutum* revealed by small-angle neutron scattering and circular dichroism spectroscopy. *Photosynthesis Research*, *111*(1-2), 71–79. https://doi.org/10.1007/s11120-011-9693-6

Park, J., Lee, J. H., & Khim, J. S. (2016). The identity of '*Berkeleya scopulorum*' from Northeast Asia: Report on *Climaconeis mabikii* sp. nov. from temperate marine waters with notes on biogeography of the genus. *Ocean Science Journal*, *51*(4), 591–598. https://doi.org/10.1007/S12601-016-0059-Z

Prasad, A. K. S. K. (2003). Fine structure and taxonomy of two species of the marine diatom genus *Climaconeis* (*Berkeleyaceae*, *Bacillariophyta*): *C. silvae* sp. nov. and *C. riddleae* sp. nov. from the Caribbean Sea and Florida Bay, USA. *Hidrobiológica*, *13*(1), 9–22.

Prasad, A. K. S. K., Riddle, K. A., & Nienow, J. A. (2000). Marine diatom genus *Climaconeis* (*Berkeleyaceae*, *Bacillariophyta*): Two new species, *Climaconeis koenigii* and *C. colemaniae*, from Florida Bay, USA. *Phycologia*, *39*(3), 199–211. https://doi.org/10.2216/i0031-8884-39-3-199.1

Puillandre, N., Brouillet, S., & Achaz, G. (2021). ASAP: Assemble species by automatic partitioning. *Molecular Ecology Resources*, *21*(2), 609–620. https://doi.org/10.1111/1755-0998.13281

Pyszniak, A. M., & Gibbs, S. P. (1992). Immunocytochemical localization of photosystem I and the fucoxanthin-chlorophyll a/c light-harvesting complex in the diatom *Phaeodactylum tricornutum*. *Protoplasma*, *166*(3-4), 208–217. https://doi.org/10.1007/BF01322783

Rambaut, A., Drummond, A. J., Xie, D., Baele, G., & Suchard, M. A. (2018). Posterior summarization in Bayesian phylogenetics using Tracer 1.7. *Systematic Biology*, *67*(5), 901–904. https://doi.org/10.1093/sysbio/syy032

Reid, G., & Williams, D. M. (2002). The marine diatom genus *Climaconeis* (*Berkeleyaceae*, *Bacillariophyta*): Two

new species from Abu Dhabi, United Arab Emirates. *Diatom Research*, *17*(2), 309–318. https://doi.org/10.1080/0269249X.2002.9705550

Ronquist, F., & Huelsenbeck, J. P. (2003). MrBayes 3: Bayesian phylogenetic inference under mixed models. *Bioinformatics*, *19*(12), 1572–1574. https://doi.org/10.1093/bioinformatics/btg180

Round, F. E., Crawford, R. M., & Mann, D. G. (1990). *The diatoms: Biology and morphology of the genera*. Cambridge University Press.

Schmid, A. M. M. (2001). Value of pyrenoids in the systematics of the diatoms. In A. Economou-Amilli (Ed.), *Proceedings of the 16th International Diatom Symposium* (pp. 1–32). Amvrosiou Press.

Tamura, K., Stecher, G., & Kumar, S. (2021). MEGA11: Molecular Evolutionary Genetics Analysis Version 11. *Molecular Biology and Evolution*, *38*(7), 3022–3027. https://doi.org/10.1093/molbev/msab120

Theriot, E. C., Ashworth, M., Ruck, E., Nakov, T., & Jansen, R. K. (2010). A preliminary multigene phylogeny of the diatoms (*Bacillariophyta*): Challenges for future research. *Plant Ecology and Evolution*, *143*(3), 278–296. https://doi.org/10.5091/plecevo.2010.418

Wood, A. M., Everroad, R. C., & Wingard, L. M. (2005). Measuring growth rates in microalgal cultures. In R. A. Andersen (Ed.), *Algal culturing techniques* (pp. 269–286). Elsevier Academic Press.

Zhang, J., Kapli, P., Pavlidis, P., & Stamatakis, A. (2013). A general species delimitation method with applications to phylogenetic placements. *Bioinformatics*, *29*(22), 2869–2876. https://doi.org/10.1093/bioinformatics/btt499